Morphodynamic modeling the impact of large-scale embankment on the large bar in a convergent estuary

Xie, Dongfeng; Wang, Zheng Bing ; van der Wegen, Mick; Huang, Junbao

Important note
To cite this publication, please use the final published version (if applicable).
Please check the document version above.
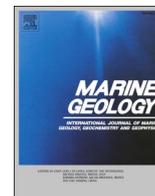
Research Article

Morphodynamic modeling the impact of large-scale embankment on the large bar in a convergent estuary

Dongfeng Xie [a,*], Zheng Bing Wang [b,c], Mick Van der Wegen [c,d], Junbao Huang [a]

[a] *Zhejiang Institute of Hydraulics and Estuary, Hangzhou, China, Zhejiang Provincial Key Laboratory for Estuarine and Coastal Research, China*
[b] *Faculty of Civil Engineering and Geosciences, Delft University of Technology, The Netherlands*
[c] *Deltares, P.O. Box 177, 2600, MH, Delft, The Netherlands*
[d] *IHE Delft, PO Box 3015, 2601, DA, Delft, The Netherlands*

ARTICLE INFO

ABSTRACT

Many alluvial estuaries worldwide include an inside bar system, a large sediment deposit deeply stretched into the estuary. A good example of such a system is the large sediment deposit in the Qiantang Estuary, China. Its length and height reach 130 km and 10 m, respectively. Bathymetrical comparison reveals that the large bar has moved seaward by around 15 km over the last decades, probably related to the large-scale coastal embankment project. This motivated a quantitative investigation of the impact of estuarine planform on the inside bar development. The bar morphology is reproduced by means of an idealized 1-D morphodynamic model. Model results suggest that the bar movement is related to a decreasing tidal prism, increasing flood dominance in the lower reach and enhanced ebb currents in the upper reach, in response to the embankment. The timescale of the morphological response is only several years. The rapid response is related to the strong tidal currents and large sediment fluxes within the estuary. Sensitivity experiments show that the location and dimensions of the bar are related to the convergence length of the estuary. A decrease of the convergence length causes seaward movement and shortening and lowering of the bar. The bar dimensions also depend on the ratio between river and tidal discharges. When the ratio increases, the bar apex moves seaward and the elevation decreases. The bar movement has significantly influenced the tidal bore in the Qiantang Estuary.

1. Introduction

Located at the transitional zone between river and the sea, estuaries are of enormous societal and environmental importance. They provide accessibility for navigation, freshwater and fertile soil of the adjacent floodplains. Therefore most densely populated areas of the world are situated near estuaries. Estuaries also play an important role in global carbon/biogeochemical cycling, and serve as a crucial feeding and breeding ground for various flora and fauna (e.g., Dyer, 1997; Townend, 2012; Savenije, 2012). The estuarine morphology is shaped by natural forcing such as river flow, tides, waves and human activities such as land reclamation, navigational training, sand mining and dam construction. Particularly in the last two centuries, anthropogenic impact has increased and has, in many cases, overwhelmed the influences of natural developments, causing many estuaries and deltas to be in a state of rapid transition (Wang et al., 2015; Hoitink et al., 2017). From the perspective of sustainable coastal management, it is of major significances to

understand and predict the morphodynamic behavior of estuaries in response to changing natural conditions and human activities.

In estuarine environments, the seaward decreasing river flow impact is coupled with the landward decreasing impact of tidal motion. There exists a certain place where seaward sediment transport by river offsets landward sediment transport by tides (Dalrymple and Choi, 2007; Choi et al., 2020). This inevitably results in the development of sediment bodies, like distributary mouth bars, river-channel bars and tidal ridges. They build up the skeleton of estuaries and play a major role in the hydrodynamics and sediment transport (Zhang et al., 2020a).

Morphodynamic models provide a powerful tool to investigate the formation and underlying physical mechanisms of observed morphological patterns in the real world. Geleynse et al. (2011); Canestrelli et al., 2013; Leonardi et al., 2013; Xie et al. (2017a); Hoitink et al. (2017) and Luan et al. (2018) are examples of recent research efforts to address mouth bar formation, and its morphodynamic response to riverine sediment supply. Van der Wegen and Roelvink (2012), Dam

* Corresponding author.
  E-mail address: dongfeng.xie@hotmail.com (D. Xie).

et al. (2016) and Nnafie et al. (2018, 2019) addressed the importance of the estuarine planform and historic land reclamation works on the evolution of the channel-shoal patterns. However, the morphodynamics of an extended inside bar, a first order morphological feature located in the inner estuary, remains relatively unexplored, especially considering their response to human activities such as land reclamations.

The Qiantang Estuary is one of the largest macro-tidal estuaries worldwide (Fig. 1). A large longitudinal bar is developed in the inner estuary. It is the largest estuarine sediment deposit in China. With a length of around 130 km, and the highest part about 10 m above the estuary's bed, its spatial scale is at least one order larger than single or complex sandbars observed in many other estuaries. The formation of this bar is due to the ample sediment supply from the adjacent Changjiang (Yangtze) Estuary, of which the fluvial sediment load used to be 450 million tons per year, and is transported along shore and into the Qiantang Estuary (Milliman et al., 1985; Chen et al., 1990; Zhang et al., 2014, Zhang et al., 2015). In recent years, several morphodynamic models have been employed to reproduce the formation of the large bar and explore the underlying physical mechanisms (Yu et al., 2012; Xie et al., 2017b; Hu et al., 2018). Based on a long series of bathymetric data in the estuary, Xie et al. (2018) suggested that under natural conditions, the morphodynamics of the Qiantang Estuary is controlled by a combination of river flow and tides, especially by river flood events and tidal bores.

Since the 1960s, a large-scale coastal embankment project (LCEP) narrowing the Qiantang Estuary has been gradually implemented (Fig. 1). The planform of the estuary has been changed considerably. Several studies have focused on the influences of the LCEP on the hydrographical regime, using water level records or numerical modeling based on shoreline changes (Zou and Shen, 2017; Jin et al., 2020). But still there exist a gap between the hydrographic change and morphological evolutions. Recent analysis of the bathymetrical data revealed
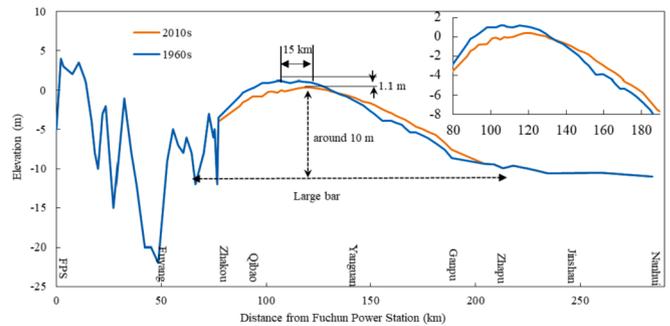
Fig. 2. The laterally averaged longitudinal bathymetries in the 1960s and the 2010s, after Pan and Han (2017).
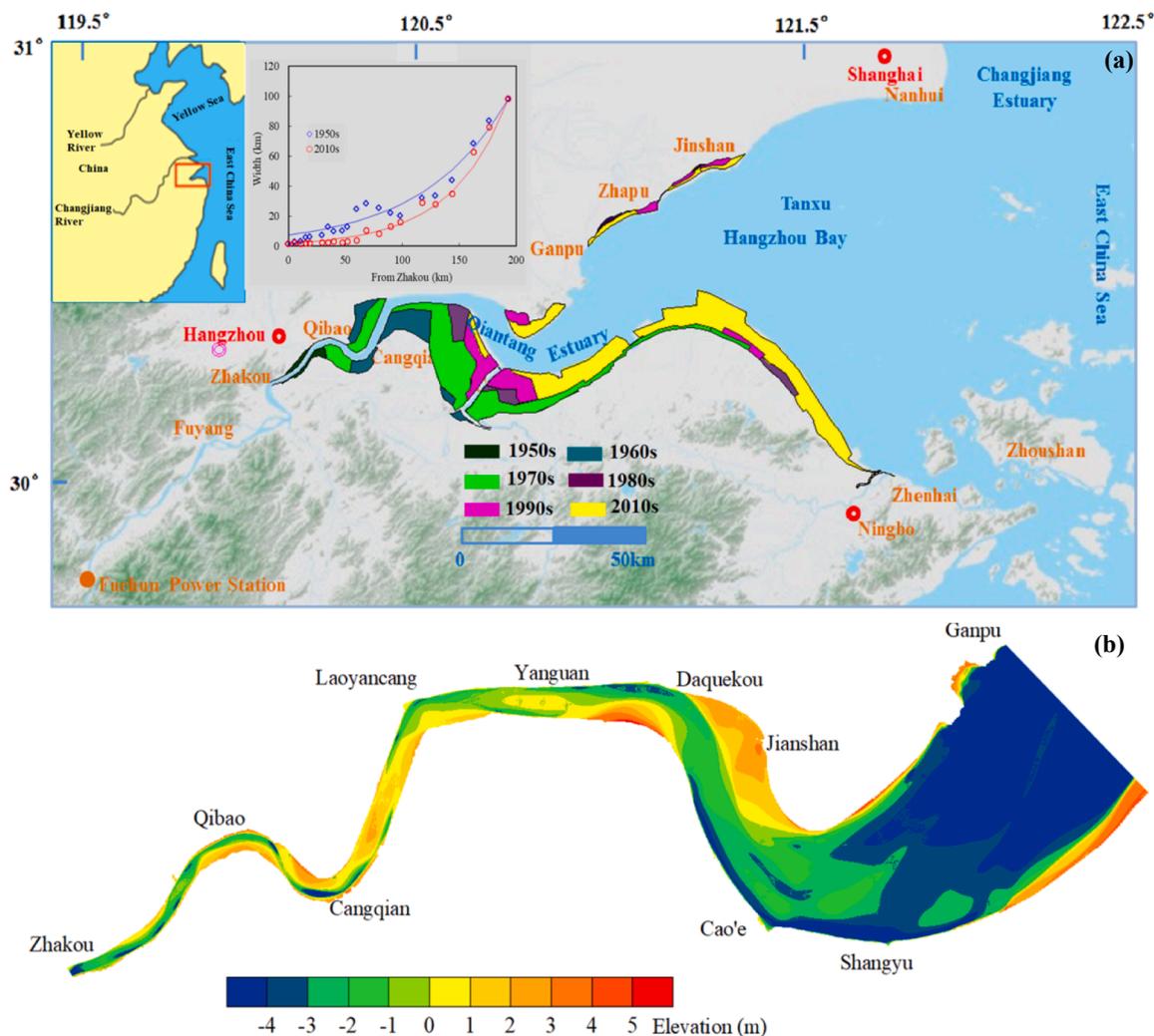
Fig. 1. (a) Location of the Qiantang Estuary; (b) bathymetry of the estuarine reach measured in November 2020. The colored shades in panel (a) indicate the progress of the large-scale coastal embankment project since the 1950s.

that the bar has shown a seaward movement in the last decades (Fig. 2). This raises scientific questions on the underlying physical processes for the bar movement and to what extent the estuarine planform can determine the dimensions of the bar within the estuary?

The large bar of the Qiantang Estuary is also the region where one of the most spectacular and fascinating tidal bore in the world occurs, a particular hydraulic phenomenon readily observed as a near-vertical wall of water traveling upriver during flood tide (Bartsch-Winkler and Lynch, 1988; Chanson, 2012). It has been long recognized that the large bar is one of the prerequisites for the bore formation (Chen et al., 1964; Chen et al., 1990; Han et al., 2003). The drastic landward rising bed level in the bar reach reduces the water depth and promotes the tidal wave deformation and eventually breaking. In recent years, several studies have focused on the turbulence properties and associated sediment transport of tidal bore based on short-term (e.g., a spring-neap tidal cycle) field observations and numerical models (e.g., Pan and Huang, 2010; Fan et al., 2014; Tu et al., 2021). However, few focused on the impact of anthropogenic morphological changes on the bore propagation.

In this contribution, we aim to explore the influence of estuarine planform on the morphological development of an inside bar, taking the large bar in the Qiantang Estuary as an example. Specific objectives are: (1) to reproduce the morphological response of the inside bar in the Qiantang Estuary to the large-scale coastal embankment works and analyze the underlying physical mechanisms; (2) to determine the controls of the bar dimensions and location and to develop a comprehensive framework of the bar morphodynamics; (3) to explore the influence of the bar evolution on the tidal bore characteristics. The Qiantang Estuary is surrounded by one of the most developed regions in China. Due to its large extent, the morphodynamic evolution of the inside bar affects the entire environment of the estuary. Therefore, studying the morphodynamic evolution of the large bar in the Qiantang Estuary not only improves our understanding of the morphodynamic behavior of the inside bar but also helps the coastal development and marine spatial planning of local government.

2. Study area

The Qiantang Estuary is a macro-tidal convergent estuary, located immediately south of the Changjiang (Yangtze) Estuary (Fig. 1). The length is 282 km and the width narrows from 98.5 km at the mouth to less than 1 km at the landward end. The estuary can be divided into three reaches (Han et al., 2003). The riverine reach, extending over 87 km upstream Zhakou to the Fuchun Power Station, is dominated by river discharge while the effects of tides are limited. It is mainly composed of coarse sand and gravel and the bed is relatively stable. The seaward reach downstream Ganpu, also well known as the Hangzhou Bay, is 87 km long and controlled by tidal currents. With the sediment input from the Changjiang Estuary, the Hangzhou Bay has continuously experienced net deposition, with an average accumulation rate of 1.15 cm over the recent 100 years (Dai et al., 2014). The estuarine reach between Zhakou and Ganpu, with a length of 108 km, is floored by easily erodible, well-sorted silt and clay floored on the bed. It is controlled by the combination of river flow and tidal currents. The morphological evolution in this reach is comparatively dynamic.

The most remarkable morphological feature of the estuary is the large longitudinal bar (Figs. 1b and 2). It starts from Zhapu at the middle Hangzhou Bay and elongates by about 130 km landward. The bed level rises gradually from about −10 m at Zhapu to 1 m at the Qibao – Cangqian reach, and then gradually decreases to be about −20 m (with respect to the Chinese National Vertical Datum of 1985, the same below). There are several bends upstream of Ganpu. The thalweg and tidal flats are developed at the concave and the convex banks, respectively (Fig. 1b). Between Zhapu and Jinshan, a large tidal channel and a tidal flat have developed in the northern and southern Hangzhou Bay, respectively (Han et al., 2003; Xie et al., 2009, Xie et al., 2017b).

Downstream from Jinshan, there is a large subaqueous plain with an average depth of about 11 m.

The annual discharge from the Qiantang River is 952 m^3/s, much smaller than the tidal prism at the mouth that can be 30 × 10^9 m^3 (tidal flow discharge in the order of 10^6 m^3/s) during spring tides (Xie et al., 2017a). Due to the monsoon climate, river discharge is characterized by seasonal and interannual variations. The period between April and July is the wet season, with an average peak value of 1893 m^3/s in June while the period between August and next March is the dry season, with a monthly discharge varying between 438 and 592 m^3/s (Xie et al., 2017b). Over the years, the annually averaged discharge fluctuates between 319 and 1390 m^3/s. During high flow season, the flood peaks can be more than 10,000 m^3/s, with the daily maximum being 12,787 m^3/s since the 1960s (Han et al., 2003). The Qiantang Estuary is strongly influenced by the river flood events and the tidal bore in the estuary, one of the largest in the world (Bartsch-Winkler and Lynch, 1988; Pan and Huang, 2010). As a result, the estuary is characterized by active morphological changes on seasonal and interannual time scales. Especially in the inner estuary the local bed level change can be more than 5 m in several months (Chien et al., 1964; Han et al., 2003; Xie et al., 2018).

The tides in the estuary originate from the East China Sea and are mainly composed of a semidiurnal M$_2$ constituent. The mean tidal range is about 3.2 m at the mouth (Xie et al., 2017a). Landward width convergence and shallower bathymetry considerably deform the tidal waves upstream evolving into the world famous Qiantang bore. The tidal range increases landward and reaches its maximum at Ganpu, with a multi-year average of 6.0 m, and then decreases landward due to bed friction. Wind waves are weak in this area, with an annually averaged wave height of 0.5 m at the Tanxu station (water depth of about 10 m) in the Hangzhou Bay (Han et al., 2003).

Due to the large width to depth ratio, the main channel of the Qiantang Estuary used to meander continuously, and the coastal protection revetments used to collapse frequently, resulting in lack of resources for development and navigation channel maintenance. Since the 1960s, a large-scale coastal embankment project has been carried out for the purpose of flood defense and land reclamation amongst others (Li and Dai, 1986; Han et al., 2003). The LCEP was implemented gradually seaward and basically finished in the 2010s (Fig. 2). The land reclamation mainly occurred at the middle and high flats. So far, more than 1000 km^2 land has been reclaimed and the planar shape of the estuary has been largely changed. For example, the width at Yanguan has decreased from about 10 km to about 2.5 km and at Ganpu from about 22 km to 18 km.

3. Model description

3.1. Model setup

The inside bar in the Qiantang Estuary is a longitudinal morphological feature, with the length much larger than the width and depth. Since the main body of the inside bar is located in the estuarine reach where the width is relatively small, the lateral variation of the morphology is less important. Therefore, a 1-D model can fulfill the controlling processes of the hydrodynamics and morphological evolution. Compared to the complex morphodynamic models that contain the state-of-the-art physical descriptions and parameterizations, an idealized model focuses on the prevailing morphological processes and favors an examination of the underlying physical mechanisms in a straightforward manner, through input reductions including simplified geometry and boundary conditions and formulations.

We construct an idealized 1-D morphodynamic model based on the Delft3D software (Deltares, 2016), which has been widely used for hydrodynamics and morphodynamics in estuarine environments (e.g., Wang et al., 1995; Hibma et al., 2004; Van der Wegen and Roelvink, 2008; Van der Wegen and Jaffe, 2014; Guo et al., 2014; Zhou et al.,

2017; Nnafie et al., 2019). Flow is calculated based on the horizontal shallow water equations. Transport of the suspended sediment is based on the advection-diffusion equation, in which the erosion and deposition fluxes between the bed and the water column are calculated by the well-known Krone-Partheniades formulation (Partheniades, 1965). Bed elevation is dynamically updated at each computational time step, based on the conservation of sediment mass and multiplied by a morphological factor of 10 to enhance bed level change.

This study focuses on the influences of changes in estuarine planform on the morphodynamic development of the large bar and associated hydrographic regime. Two basic cases are set. The model domain mimics the outlines of the Qiantang Estuary in the 1950s and the 2010s, representing the estuarine planforms before and after the LCEP, respectively (Fig. 3). The domain consists of a 280 km long basin with a constant width of 1 km for the first 90 km followed by a width expanding to 100 km at the mouth. Compared to the 1950s case, the coastline in the 2010s case is narrowed by 8 km at 140 km and 4 km at 200 km (the x-coordinate is defined from the landward end, as shown in Fig. 3a). The initial bed level decreases linearly from 0 m at the landward end to -9 m at the seaward end, indicating a preliminary longitudinal bed slope of 3.2×10^{-5}.

At the seaward boundary, the model is forced by a semidiurnal M_2 tide with a tidal amplitude of 2 m. A suspended sediment concentration (SSC) of 1.0 kg/m^3 is prescribed, close to the annual average SSC at the mouth (ECCHE, 1992; Xie et al., 2017a). At the landward boundary, episodic river flood events are neglected so that we can focus on the long-term morphologic development of the large bar under human activities. A constant river discharge of 1000 m^3/s is prescribed, close to the annually averaged discharge from the Qiantang River. The SSC is set to be 0.15 kg/m^3, denoting that the annual sediment supply from the Qiantang River is about 5×10^6 ton (Chen et al., 2006). Both the two cases are run for 3 years of morphodynamic evolution in which the bar system is formed. As a first approximation, we neglect the role of salinity stratification.

3.2. Model runs for sensitivity analysis

In order to obtain a more general understanding of the controls of the planform of the estuary on the bar dimensions, an additional group of numerical experiments is conducted (Table 1). The formulation of estuary convergence with a width reducing exponentially in landward direction has been well adopted in many studies and can be expressed by the following classical relation (e.g., Friedrichs and Aubrey, 1994; Lanzoni and Seminara, 1998; Savenije, 2012):

$$B = B_0 exp\left(-\frac{L - x}{L_b}\right) \tag{1}$$

in which B_0 is the width at the mouth, L is the estuary length and L_b is the convergence length. Based on the widths along the estuary in the 1950s and 2010s (upper right panel in Fig. 1a), it can be found that the convergence length of the estuary has decreased from 65 km to 50 km, indicating an increase of the convergence. The width at the estuary mouth is fixed at 100 km, since it is determined by the geological background such as the Zhoushan archipelago. The width along the estuary is decreased exponentially landward with convergence lengths of 20, 40, 60, 80, 100 km, respectively. The other model inputs are kept invariant.

In an alluvial estuary, river discharge and the associated sediment

Table 1
Overview of model input variations in the sensitivity analysis.

Group	Estuary planform	River discharge
1	Based on shoreline in the 1950s and 2010s	1000 m^3/s
2	L_b = 20, 40, 60, 80, 100 km	1000 m^3/s
3	Based on shoreline in the 1950s	250–2000 m^3/s, with an interval of 250 m^3/s
4	Based on shoreline in the 2010s	250–2000 m^3/s, with an interval of 250 m^3/s
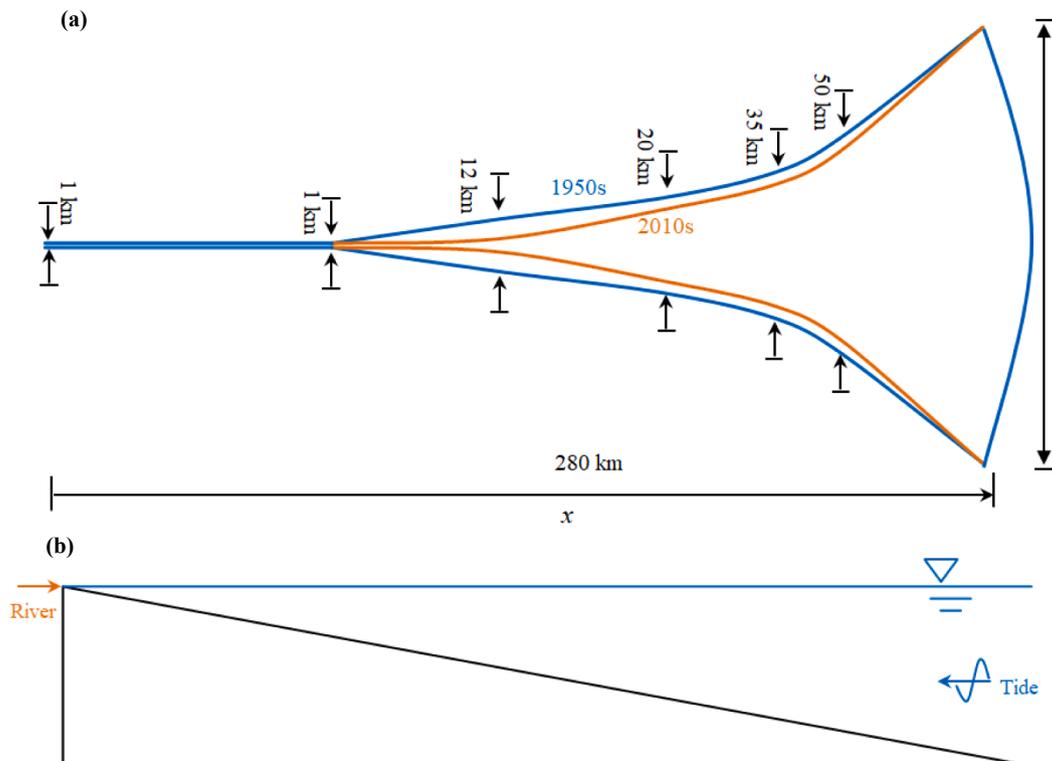
Fig. 3. Sketch of the modeled estuary. (a) Geometry (top view); (b) initial bathymetry (side view).

supply may play an important role, especially in the upper reach where smaller channel cross-sections and tidal prisms prevail. River flows attenuate tidal currents through enhanced tidal friction, and constrain landward saltwater intrusion by enlarging ebb currents (Godin, 1985; Savenije, 2012; Hoitink and Jay, 2016). As a result, considerable morphological changes in estuarine environments may take place due to the variations of river discharges. In terms of the Qiantang Estuary, it has been recognized that during the high flow periods, the river flow erodes the bed and transports sediment seaward whereas during the low flow periods, the tidal currents transport sediment landwards leading to deposition in the inner estuary (Han et al., 2003; Xie et al., 2017b; Xie et al., 2018). In this study, in order to explore the controls of river discharge on the bar dimensions, a series of sensitivity runs are added on the basis of the two basic cases, with the river discharge varying from 250 to 2000 m³/s with an interval of 250 m³/s. These values fall in the reasonable range of the river discharges of the Qiantang River, as mentioned in the previous section.

4. Model results

4.1. Morphological evolution

Fig. 4 illustrates the processes of the morphological evolution of the estuary in the 1950s and 2010s cases. In the model the large bar is formed in 3 years, in agreement with recent studies (Xie et al., 2017b; Hu et al., 2018). In the 1950s case, the reach upstream 50 km has significantly eroded. The sediment is transported seaward. The cumulative sediment transport through the 50 km transect over 3 years is 5.7 × 10⁶ m³. The reach downstream 175 km is eroded, tending to evolve toward a subaqueous plain, and the sediment is transported landward. The cumulative sediment transport through the 175 km transect over 3 years is 57.5 × 10⁶ m³. As a result, sediment of 63.2 × 10⁶ m³ is accumulated between 50 and 175 km, and a large bar is gradually developed. More than 90% of the sediment accumulated in the bar region is from seaside, consistent with previous studies on the sediment sources of the large bar (Chen et al., 1990; Zhang et al., 2015). The bar apex is located at 103.5 km and its elevation is 1.10 m. Morphological development in the 2010s case is similar. The bar apex is located at 122.4 km and its elevation is 0.54 m. The cumulative sediment accumulation at the bar area is 58.0 × 10⁶ m³, smaller by 5.2 × 10⁶ m³ than that in the 1950s case. Compared to the 1950s case, the bar apex in the 2010s case has moved seaward by 16 km and lowered by 0.86 m. The landward slope of the bar (upstream the apex) is eroded by 1.5 m on average whereas the seaward slope (downstream the apex) is accumulated by 1.0 m on average.

Overall, the simulated longitudinal profiles after 3 years are comparable with the real situations (Fig. 3), indicating that the model can skillfully reproduce the morphological response of the bar to the LCEP. Furthermore, the longitudinal length of the bar has decreased from
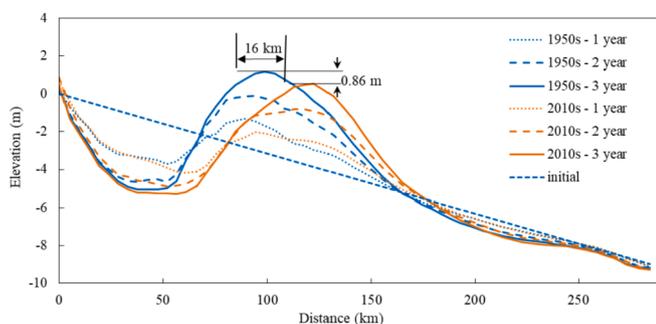
137.3 km to 128.8 km. This is mainly related to the seaward movement of the landward slope of the bar, because the location of tail of the bar has hardly changed.

Similar to the 2-D morphodynamic modeling of Xie et al. (2017b), a longer than 3 year simulation shows that the bar grows continuously to an unrealistic height (≫10 m). In reality, the growth will be constrained by erosion during high river discharge periods, i.e. river flood events. In the Qiantang Estuary, flood events occur almost in each year (Han et al., 2003). Flood events erode seriously the bed in the inner estuary and export sediment seaward. Over a long enough time span, the sediment input by tides can be balanced by sediment export by flood events (Xie et al., 2017b; Xie et al., 2018).

4.2. Hydrodynamic and sediment transport changes

The hydrodynamics and associated sediment transport are responsible for the morphological dynamics in estuaries. Exploring the origin of the large bar in the Qiantang Estuary (Yu et al., 2012; Xie et al., 2017b; Hu et al., 2018) suggested that landward sediment transport by flood dominance is the main cause for the bar formation. Here we focus on the change of the hydrodynamic regime induced by the change of the estuarine planform.

In the initial state, both the high and low water levels increase landward due to backwater effects (e.g., Savenije, 2012; Hoitink and Jay, 2016) (Fig. 5a). The tidal range maintains around 4 m downstream of 90 km and decreases gradually landward due to the bed friction. The tidal bore is also reproduced (Fig. 5b). After the coastal embankment, the high water level increases upstream 150 km due to the enhanced reflection of the tidal wave. The maximum increase is about 0.5 m. The low water level increases upstream 100 km but decreases between 100 and 220 km. Subsequently, the tidal range upstream 200 km is increased, with the maximum being 0.6 m.

Both flood and ebb velocities increase between 50 and 250 km, because the narrowing of the estuary converge the tidal energy. The maximum increase of the velocities appears at around 100 km (Fig. 5c). Between 50 and 250 km, the flood maximum (u_f) is larger than ebb maximum (u_e), with a maximum ratio of u_f/u_e of 1.74, indicating the flood dominance (Fig. 5d). Downstream 50 km and upstream 250 km, the flood maximum is less than ebb maximum, indicating the ebb dominance. After the coastal embankment, the flood dominance decreases upstream 90 km and increases downstream 90 km. Overall, the changes of the flood and ebb velocities induced by the embankment works are qualitatively consistent with the results of Zou and Shen (2017) who simulated the influences of the LCEP on the hydrodynamics in the estuary using real coastline and bathymetry.

The tidal prism Q_t, the ratio R between the river discharge and the tidal prism along the estuary are calculated as follows:

$$Q_t = \int_{t_0}^{t_0+T_f} UHBdt \tag{2}$$

$$R = \frac{\int_{t_0}^{t_0+T_f} qdt}{Q_t} \tag{3}$$

where U is the depth-averaged current velocity (m/s), H is the water depth (m), B is the width (m), t_0 is the begin of flood period, T_f is the flood duration (s), q is river discharge (m³/s). The sediment fluxes of flood and ebb tides are function of the tidal prism, SSC and river discharge.

The tidal prism at the estuary mouth is about 28 × 10⁹ m³ and decreases gradually landward (Fig. 5e), in agreement with the field observation (Xie et al., 2017a). Correspondingly, the ratio R decreases from 0.18 at the landward end to less than 0.001 at the seaward end. After the embankment, the tidal prism decreased by about 30%. Hence the ratio R is increased accordingly (Fig. 5f). Sediment flux at the mouth is about 2.2 × 10⁶ m³ and increases slightly landward but then decreases

Fig. 4. Modeled bathymetries of the bar at the bar formation (a) and the development of the longitudinal profiles of the estuary. The arrows across 50 km and 175 km denote the directions of the cumulative sediment transport over 3 years.
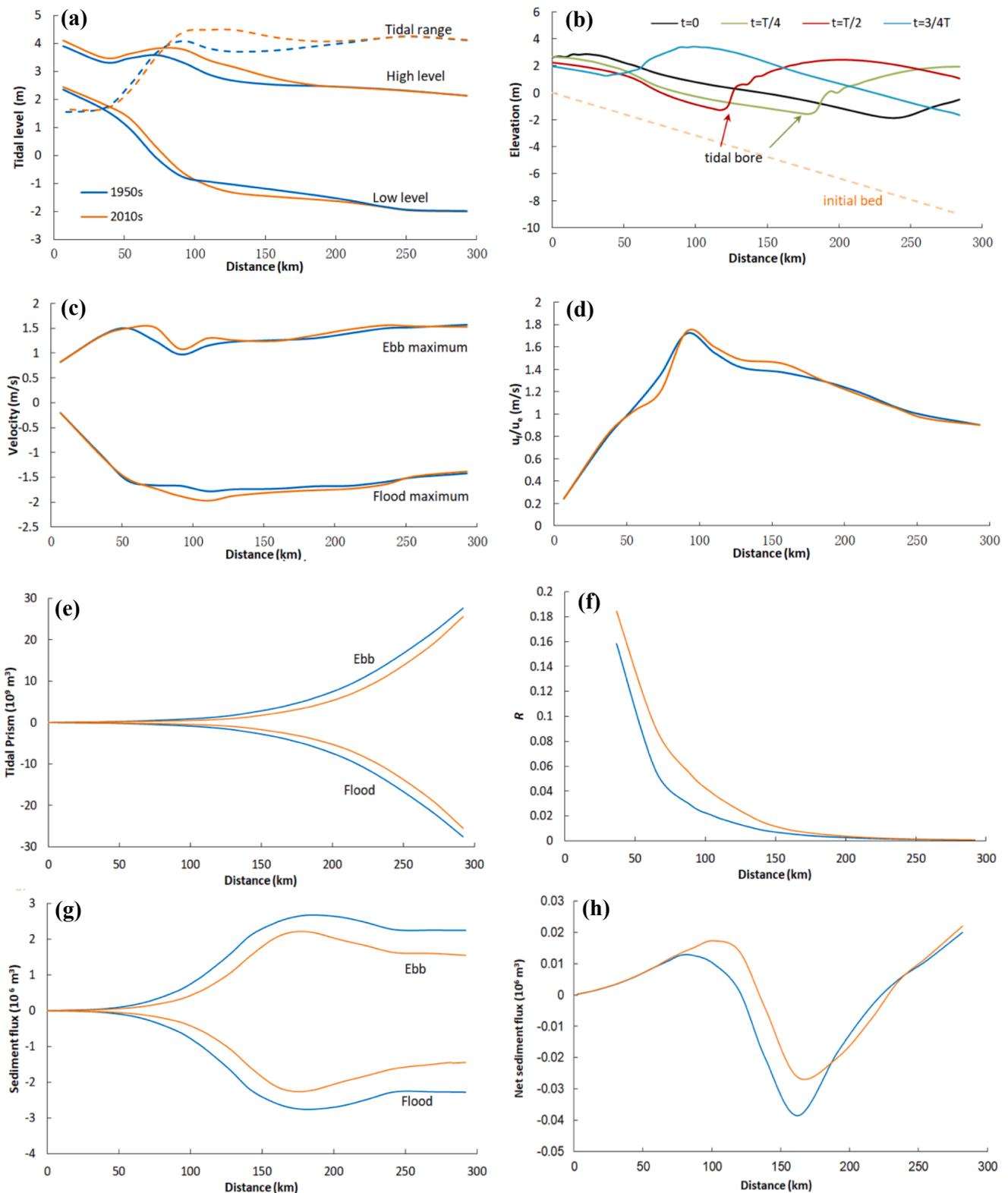
Fig. 5. Hydrodynamics and sediment transports along the estuary at the initial states. (a) High, low tidal levels and tidal ranges, (b) the water levels at four instants in the 2010s case, (c) maximum flood and ebb velocities, (d) the ratio between maximum flood velocity to maximum ebb velocity, (e) flood and ebb water fluxes over one tidal cycle, (f) the ratio between river flow and prism, (g) cumulative sediment transport and (h) the net sediment transport over one tidal cycle.

(Fig. 5g). The net sediment flux is in the order of 10^4 m^3 per tidal cycle, being negative between 90 and 200 km, and positive upstream 90 km and downstream 250 km (Fig. 5h). Since the bed level change is related to the spatial gradient of sediment transport rate, sediment will accumulate in the bar area. After the embankment, the changes of sediment

fluxes are similar to those of tidal prisms. The sediment flux downstream 150 km decreases by about 20%. The net sediment transport decreases between 100 and 170 km whereas increases between 170 and 250 km.

In the region of bar formation, both the high and low water levels upstream 100 km is lowered due to the bed erosion in the upper reach

(compare Figs. 5a and 6a). The longitudinal water level slope is decreased accordingly. The difference between the high levels in the two cases is comparable with that at the initial stage, indicating that the influence of the bathymetrical change is limited and the change of the high level is mainly related to the embankment. The low water level in the 2010s case is about 0.1 m lower than in the 1950s case, consistent with the recent finding based on field data by Jin et al. (2020) who found that the annual low levels at Zhakou, Qibao and Yanguan stations have shown decreasing trends since 1960s, with the magnitude between 0.05 and 0.2 m. This is because the low level in the upper reach is mainly related to the local bel levels (Han et al., 2003). The bed erosion of the upper reach in the 2010s case is more apparent that in the 1950s case (Fig. 4). The low level in the bar region is apparently influenced by the bathymetry, and a fast lowering of the low level occurs from 100 km to 160 km. The low level between 100 and 160 km is 0.1–0.4 m higher in the 2010s case than in the 1950s case, due to the accumulation in the downstream slope of the large bar. As a result, the tidal range in the inner estuary increases by about 0.4 m (Fig. 6b), consistent with field data (Pan and Han, 2017). Such a tidal amplification is similar to the sand extraction in the Pearl Estuary, Southern China and and channel deepening in the Ems Estuary (Zhang et al., 2010; Van Maren et al., 2015; Dijkstra et al., 2019). However, the tidal amplification in the Qiantang Estuary is not directly induced by human activities but indirectly by the response of the morphodynamic system to the LCEP.

In both cases, the ebb maximum in the inner estuary decrease due to the bed erosion (Fig. 6c). Compared to the velocities in the 1950s case, both the flood and ebb maximum increase between 50 and 130 km. Subsequently, the ratio u_f/u_e increase upstream 100 km, consistent with the tidal amplification. The peak of u_f/u_e still appears in the bar area, but its location moves seaward by 18 km (Fig. 6d).

4.3. Influence of river discharge

Fig. 7 shows an example of the longitudinal profiles of the estuary in the basic cases under the variation of river discharge, and the corresponding bed level changes under the low (500 m³/s) and high (1500 m³/s) discharges, compared with that under the intermediate flow (1000 m³/s). In the low flow cases, sediment accumulation and erosion occur in the upper and lower parts of the bar, respectively, and subsequently the bar moves landwards. Vice versa in the high flow cases. The magnitudes of bed level change in the high flow case is smaller than in the low flow case, implying the bed level change is more sensitive to the river discharge variation in the low flow period.

Compared to the 1950s case, the region with significant bed level changes in the 2010s case moves seaward by about 10 km. For example, in the 1950s case, the transitional point between erosion and accumulation is located at 124 km and 132 km under the discharge of 500 m³/s and 1500 m³/s, respectively; whereas in the 2010s case it is at 132 km and 140 km, respectively (Fig. 7b). Chen et al. (1990); Han et al. (2003) suggested continuous water and sediment exchange between the estuary and the Hangzhou Bay. Our model results suggest that this exchange has changed as a result of the LCEP and the seaward movement of the large bar.

The location and elevation of the bar apex correlates well with the river discharge (Fig. 8). With the river discharge increasing from 250 m³/s to 2000 m³/s, the bar apex in the 1950s case moves seaward from 89.3 km to 109.1 km and its elevation is lowered from 2.81 m to −0.66 m. Chen et al. (1990) found similar correlations by using bathymetrical and discharge data before the beginning of the LCEP. These correlations suggest the existence of a dynamic equilibrium for the large bar, with seasonal and interannual variations depending on river discharge variations, but in balance over longer time scales. This dynamic equilibrium was also found by Fan et al. (2016) based on time-series of satellite images of the seasonal and multi-year variations of channel morphology. With the implementation of the LCEP, the correlations have been changed. On average, the location of the bar apex in the 1950s and 2010s cases is at 101.4 km and 117.0 km, respectively, and the elevation of the bar apex is 0.80 m and 0.49 m, respectively.
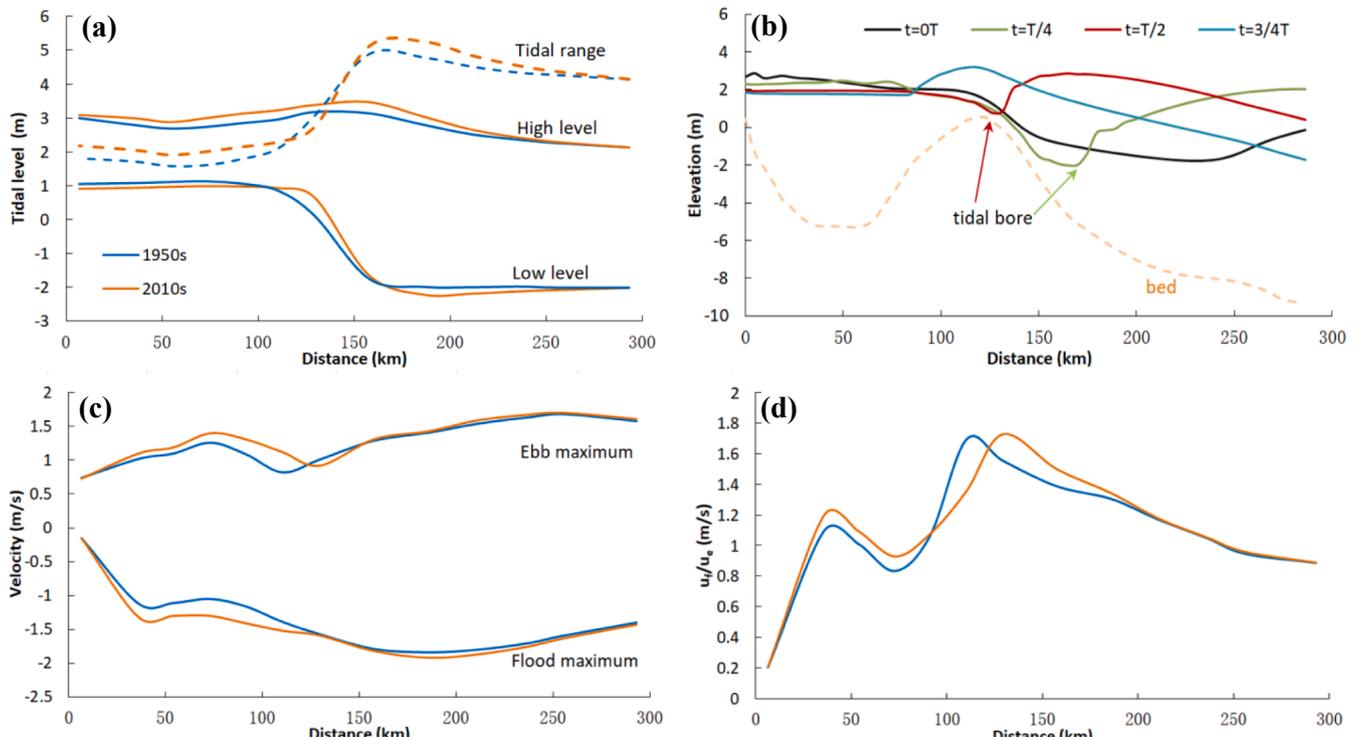
Fig. 6. Hydrodynamics along the estuary after 3 years. (a) High, low tidal levels and tidal ranges, (b) the water levels at four instants in the 2010s case, (c) the maximum flood and ebb velocities, and (d) the flood and ebb maximum ratio.
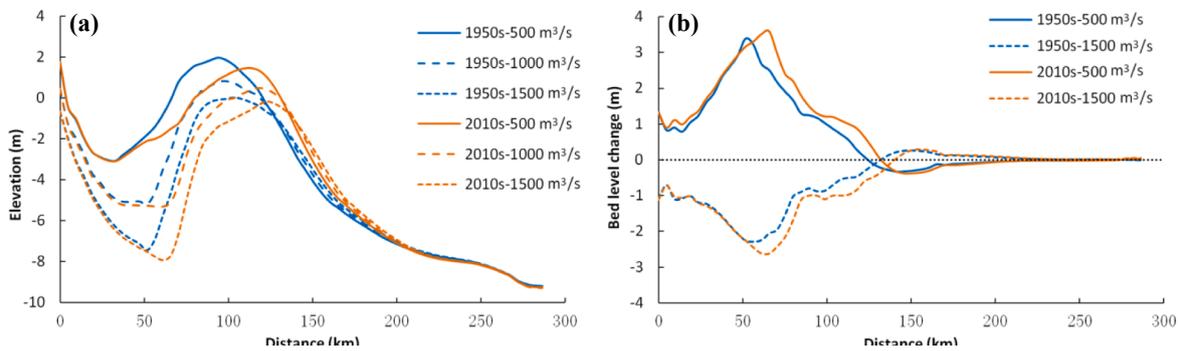
Fig. 7. Longitudinal profiles for various river discharges after 3 years (a) and the bed level changes compared to that of 1000 m³/s cases (b).
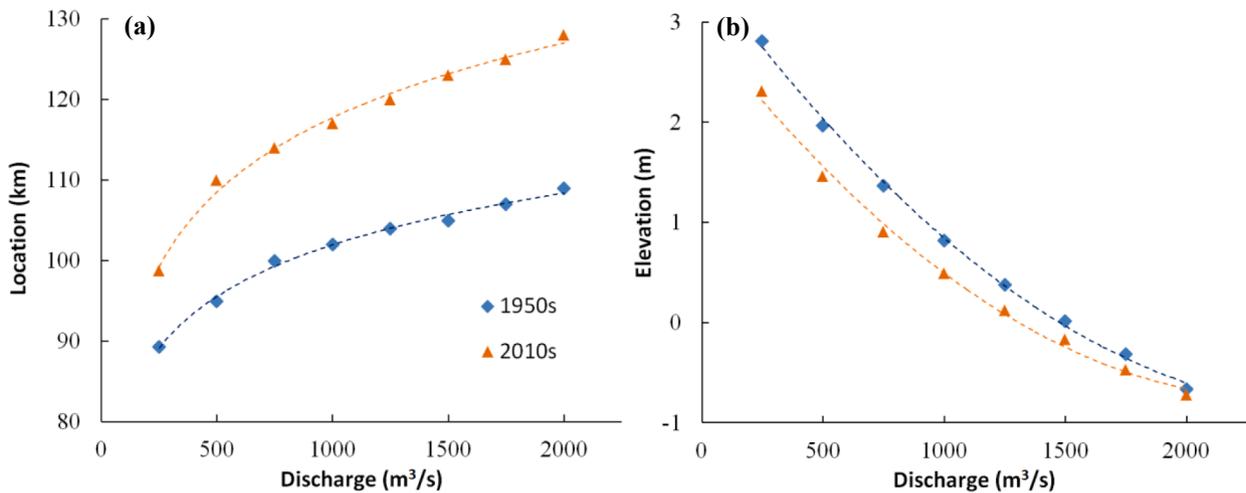
Fig. 8. Simulated correlations between the location (a) and elevation (b) of the bar apex and the river discharge.

4.4. Influence of estuary convergence

Tidal prism depends on the estuarine planform to a large extent. One of the most important consequences of land reclamation is the reduction of tidal prism (e.g., Friedrichs and Aubrey, 1994; Lanzoni and Seminara, 1998; Todeschini et al., 2008; Pye and Blott, 2014; Wang et al., 2015). Fig. 9a shows that the tidal prism at the estuary mouth correlates with the convergence length of the estuary. With the L_b decreasing from 100 km to 20 km, the prism decreases from 27.4×10^9 m³ to 12.1×10^9 m³. Accordingly, the ratio R increases (Fig. 9b). The maximum ratio for the cases of 20, 40, 60, 80 and 100 km are 2.8, 1.87, 1.40, 0.81 and 0.51,

respectively. The ratio shows a rapid reduction seaward in the upper reach (0–50 km) and then a relatively gentle reduction in the lower reach.

Fig. 10 illustrates the bathymetries of the estuary under various convergence lengths. In all cases, the large bar evolves. With a decreasing convergence length, the bar moves seaward and becomes lower, consistent with the basic cases (Fig. 4). The apex location moves from 191.8 km to 60.4 km, and elevation of the apex decreases from 3.2 m to −6.7 m, if the convergence length decreases from 100 km to 20 km. Moreover, the bar length decreases from 117.2 km to 4.6 km. Clear power or logarithmic relationships exist between the bar location as well
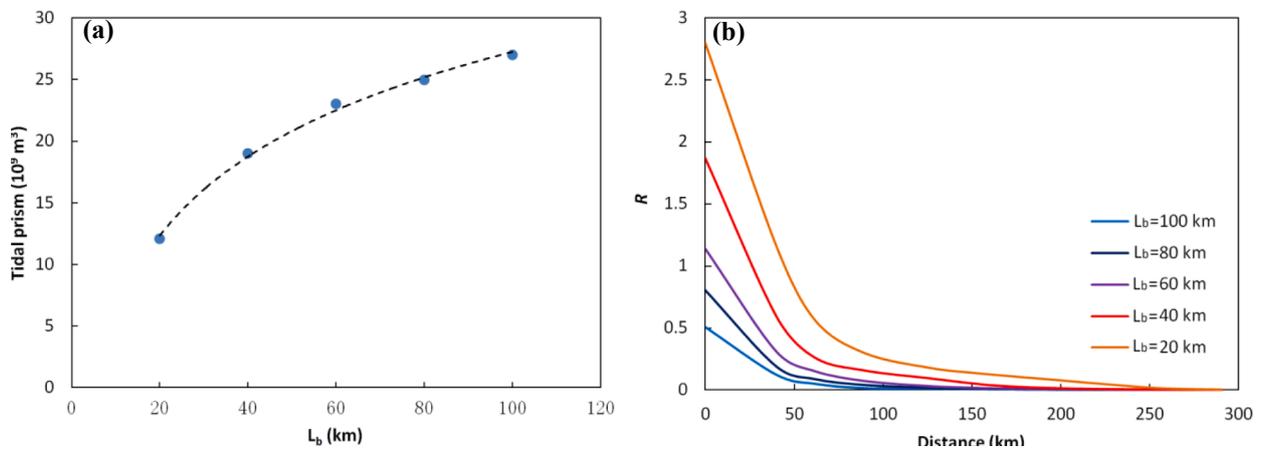
Fig. 9. Influences of the convergence length on the tidal prism at the estuary mouth (a), and the river flow - prism ratio along the estuary (b).
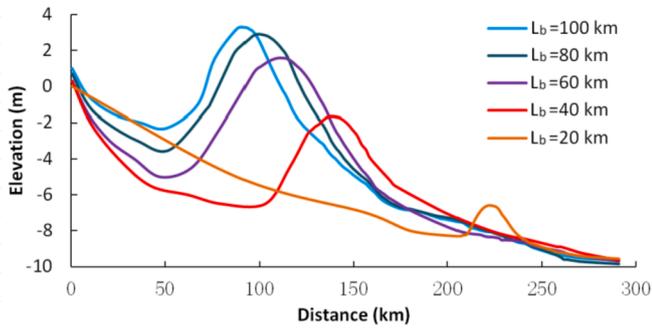
Fig. 10. The cross-sectional averaged longitudinal profiles at the bar formation for the cases of various estuary convergence.

as dimensions (elevation of the bar apex and the bar length) and the convergence length (Fig. 11).

The formation of a tidal bore is related to the tidal range at the mouth, the funnel shape of the estuary which constraints the incoming tide and converges the tidal energy, and the subaqueous bathymetry which promotes the deformation of tidal wave (Lin, 2008; Dolgopolova, 2013; Bonneton et al., 2015). The strength of the tidal bore can be quantified using the relative Froude number F_r (Peregrine, 1966; Chanson, 2011):

$$F_r = \frac{c - u_1}{\sqrt{gh_1}} \tag{4}$$

where c is the propagation speed of the bore, u_1 and h_1 are the current velocity and water depth prior to the arrival of the bore, respectively, and g is the gravitational acceleration. For $F_r > 1.5$–1.7 the bore is breaking, while for $1.3 < F_r < 1.5$–1.7 the bore is undular with limited breaking. By incorporating the analytical formula for the propagation speed of a bore (Pan et al., 2008) and formula (4), Zhang et al. (2020b) suggested the relative F_r can be calculated based on the local tidal range Δh and the current velocity prior to the bore h_u:

$$F_r = \sqrt{\frac{1}{2}\left(\frac{\Delta h}{h_u} + 1.5\right)^2 - \frac{1}{8}} \tag{5}$$

Fig. 12 shows the relative Froude number along the estuary after the bar formation in the cases of varying convergence length. Overall, the reach where F_r is larger than 1.7 is consistent with the morphological bulge of the bar, suggesting the importance of the bar on the tidal bore development. Similar to the development of the bar in the cases of various convergence lengths, the "bore reach" also shows a seaward movement. This is consistent with the observations and would be discussed below. Furthermore, the peak of F_r decreases with the decrease of

Fig. 11. Correlations between the bar dimensions and the convergence length.
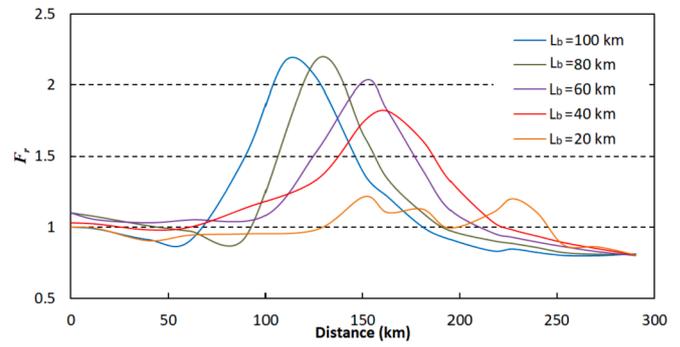
Fig. 12. Relative Froude number along the estuary after 3 years in the cases of various convergence lengths.

the convergence length. The peak is 2.18, 2.17, 2.03, 1.75 and 1.41, respectively for the 5 convergence cases in order. This indicates that the tidal bore tends to be weakened with a narrowing of the estuary. A breaking bore would disappear while only an undular bore is formed if L_b is less than 20 km.

5. Discussion

5.1. What determines the inside bar location and dimensions?

Estuarine morphology results from an intricate balance between fluvial and marine processes (Dyer, 1997; Dalrymple and Choi, 2007). The relative strength of tidal prism and river discharge is often used to be a metric for the first-order estimate of estuarine morphology. For example, downstream channel widening can be quantified by the ratio of the tidal and fluvial discharges (Nienhuis et al., 2018). Using a morphodynamic model of an idealized short estuary, Bolla Pittaluga et al. (2015) showed that the estuarine channel-bed slope tends to increase with decreasing fluvial discharge. The physical mechanism for the formation of the large inside bar in the Qiantang Estuary is also related to the ratio between the river flow and tidal prism. The planform of an estuary is one of the most important parameters controlling hydrodynamic and morphodynamic processes. Channel convergence causes a distortion of the tidal wave, strongly affects the hydrodynamics and forces the sediments to move toward the inner part of the estuary (e.g., Friedrichs and Aubrey, 1994; Lanzoni and Seminara, 1998; Todeschini et al., 2008; Savenije, 2012). Given the fact that the river discharge is invariable in the last decades, the river flow - tidal prism ratio R depends on the variation of the tidal prism. Especially the decrease of the convergence length induces a reduction of tidal prism at the estuary mouth and subsequently an increase of the ratio R (Figs. 5e and 10a). Hence the role of river discharge in the inner estuary is relatively increased, which can push the large bar seaward. Furthermore, sensitivity analysis by numerical experiments show that not only the bar location but also the bar elevation and bar length correlates well with the estuary convergence. On the other hand, when the planform of the estuary is fixed, the bar dimensions are influenced largely by the variations of the river discharge. The role of river discharge turns out to be more apparent in the case of stronger convergence of the estuary (Figs. 6 and 7).

Tidal asymmetry is an important indicator for the sediment transport and morphological pattern development (Wang et al., 2002; Van der Wegen and Roelvink, 2008; Guo et al., 2014; Zhou et al., 2018). The middle reach of the estuary is characterized by flood dominance (Fig. 5d). With the narrowing of the estuary, such reach is moved seaward slightly, and the area of sediment accumulation moves seaward (Fig. 5h).

Model results in this study show that the seaward movement of the bar induced by the LCEP has led to significant accumulation of the seaward slope of the bar (Fig. 4). Actually the accelerated accumulation
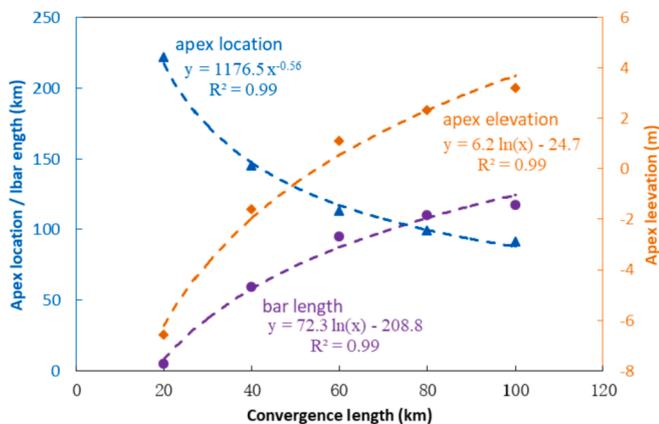
rate can extend to the inner Hangzhou Bay. Based on historical bathymetries in the Hangzhou Bay, Xie et al. (2017c) found the accumulation rate in the inner Hangzhou Bay (between Jinshan and Ganpu) has been apparently increased from 2.4 cm/a during the period of 1959–2003 to 13.4 cm/a during the period of 2010–2014. The inner Hangzhou Bay can be seen as the tail of the large bar (Fig. 2). Hence the model results explain the physical mechanism of morphological development since the 1960s in the Qiantang Estuary as well as the inner Hangzhou Bay.

Besides the estuarine planform, sediment supply is another potential factor for the morphological development. The Qiantang Estuary is one of the sinks of the Changjiang River sediment (Milliman et al., 1985; Chen et al., 1990; Zhang et al., 2014, 2015). In recent years, sediment load of the Changjiang River has been decreasing sharply from more than 4.5×10^8 t/a to less than 1.5×10^8 t/a due to soil conservation and dam constructions in the Changjiang River basin, especially since the impoundment of the Three Gorges Dam in 2003 (Gao and Wang, 2008; Yang et al., 2011; Milliman and Farnsworth, 2011; Dai et al., 2016). As a result, the Changjiang Estuary has shifted from a sediment sink to a sediment source (Yang et al., 2011; Dai et al., 2018; Mei et al., 2018; Dai, 2021). Hydrological surveys by Xie et al. (2017a) revealed that the annually-averaged net sediment flux into the Hangzhou Bay mouth has decreased slightly by about 10% after 2003. The slight decrease sediment supply at the bay mouth caused the erosion in the outer bay in recent years (Dai et al., 2014; Xie et al., 2017c). However, its influence on the inner bay and the Qiantang Estuary has been overwhelmed by the large-scale embankment project, because the erosion of the outer bay provides a sediment source for the inner bay (Xie et al., 2017c). It can be concluded that the morphological adjustment of the large sand bar in the Qiantang Estuary in the last decades is mainly related to the LCEP.

5.2. The rapid response of the bar to the estuary narrowing

Coastal embankment works can be carried out in a relatively short period, whereas the morphological response of the estuary is relatively slow (Wang et al., 2015). In most estuaries the timescale for the morphology to adapt to the new hydrodynamic conditions is usually in the order of decades to centuries (Van der Wegen and Roelvink, 2012; Nnafie et al., 2018). The narrowing project of the Qiantang Estuary started in the earlier 1960s and basically finished in the 2010s. The project was implemented gradually seaward by several stages as shown in Fig. 1a. The morphology of the estuary has been changed sequentially (Pan and Han, 2017). For a long-term morphodynamic modeling the initial bathymetry and the specific process of the narrowing may influence the formed morphological patterns to a certain extent (Van der Wegen and Roelvink, 2008; Zhou et al., 2017; Nnafie et al., 2019). In this study, we excluded the actual process of the project implementation by using simplified planforms and the same initial bathymetry before and after the LCEP, in order to focus on the influences of estuarine planform and the first-order controls of the large bar.

It turned out that the timescale of morphological response in the Qiantang Estuary is only several years, one or two orders faster than most other estuaries (Xie et al., 2017b; Hu et al., 2018). The timescale for the morphological evolution is related to the sediment transport rate (Van Rijn, 1993). The Qiantang Estuary is characterized by the strong tidal currents, especially influenced by the tidal bore, which result in large sediment transport rate (Han et al., 2003; Pan and Huang, 2010; Fan et al., 2014; Xie et al., 2018). Field observations showed that sediment flux over a flood or ebb period at the Ganpu transect is in the order of 10^6 m^3 (Han et al., 2003) and during normal river discharge periods the sediment accumulation in the estuarine reach can be in the order of 10^6 m^3 in several months (Xie et al., 2018), in agreement with the present model results.

To the authors' knowledge, the Sittaung Estuary, Myanmar, is the only macro-tidal estuary comparable with the Qiantang Estuary in terms of the fast morphodynamic adaptation rate. The length of the estuary is

220 km, and it is also funnel-shaped. Sediments are also constituted by silt and clay with median grain size ranging between 0.02 and 0.04 mm (Shimozono et al., 2019; Choi et al., 2020). Recently, Ahmed et al. (2019) reproduced the morphological patterns in the Sittaung Estuary using a morphodynamic model. Starting from an initial bed with a constant slope, the channel-shoal pattern in recent years was reproduced well with a calculation time of only several months.

5.3. The influence of the bar evolution on the tidal bore

The Qiantang Estuary is characterized by one of the biggest tidal bores in the world. The bore scenes attract millions of tourists each year. It is also an important cultural resource, symbolizing the local people's spirit of trendsetter. Therefore, to what extent the LCEP influences the Qiantang bore is one of great interests to coastal scientists, engineers and managers.

Historically, the location of the bore occurrence was further west than the present age. For example, in the Song Dynasty, about 1000 years ago, the location used to be upstream of Wenyan, about 70 km upstream of Yanguan (Chen et al., 1964). Presently the most spectacular tidal bore occurs at the Yanguan reach (Lin, 2008; Pan and Huang, 2010; Tu et al., 2021). In recent years, a breaking bore has been frequently witnessed at Shangyu, about 40 km downstream of Yanguan, indicating that the place of the bore occurrence has probably moved further seaward.

However, aside from the historical documents of the Qiantang bore, field records of the bore are very scare, making it difficult to link the bore formation with the long-term morphological evolution. Based on scale model experiment, Zeng et al. (2017) suggested that embankments near Jianshan, about 10 km long and 2.5 km wide, resulted in an increase of about 0.1 m of the bore height, due to the enhancement of the tidal wave reflection. They also suggested that if a larger embankment is carried out, the tidal prism from the East China Sea will be decreased and hence weaken the Qiantang bore. Recently, based on numerical models, Zhang et al. (2020b) and De Ridder (2017) tested the influences of the bathymetrical changes on the tidal bores in the Qiantang Estuary and the Sittuang Estuary, respectively. Increasing or reducing the bed elevation in the estuaries by a uniform value, their results showed that the bathymetry plays an important role in the bore formation and propagation. In this study, we reproduced the morphological response of the bar to the LCEP and predicted the bar location and dimensions under further narrowing in the future. It turned out that with the change of the estuarine planform and the seaward movement of the large bar, the reach for breaking bore conditions moves seaward. This explains the physical mechanisms for the historical and recent evolutions of the place of the bore occurrence. It is notable that if the estuary is narrowed further in the future, the place of the bore occurrence would move further seaward, and would be even in danger of disappearing (Fig. 12). For the estuarine regulation in the future, attention must be paid to the influence of the morphological evolution on the tidal bore.

The tidal bore is highly influenced by the bar morphology. In turn, the tidal bore also exerts great impact on the bar morphology because of the associated strong currents and sediment transport capacity. The results of the present morphodynamic model show that in addition to the seaward movement of the large bar due to the estuary narrowing, the "bore reach" also shows a seaward moving trend. It can be concluded that the morphologically active reach in the Qiantang Estuary which is strongly influenced by the bore has moved seaward in the last decades.

6. Conclusions

This study focused on the controls of the inside bar location and dimensions, taking the Qiantang Estuary as an example. Using idealized model geometries mimicking the planforms of the Qiantang Estuary in the 1950s and the 2010s, the morphological response of the large bar to the large-scale coastal embankment project was reproduced first, and

then sensitivity analyses of the convergence length of the estuary and the variations of river discharge were carried out.

The morphological response of the large bar to the narrowing project is only several years. The rapid response is related to the strong tidal currents and large sediment fluxes. With the large-scale narrowing project of the Qiantang Estuary, the apex of the large inside bar has moved seaward by 15 km and lowered by 0.86 m. For the first-order estimation of the morphology, the seaward movement can be attributed to the increase of the ratio between river flow and tidal prism at the mouth. The tidal prism correlates with the estuarine planform under a similar tide. A shorter convergence length results in a decrease of tidal prism, and an increase of the ratio between river discharge and tidal prism. The bar movement is also related to the change of tidal asymmetry along the estuary and subsequently the change of net sediment transport over a tidal cycle.

The locations, length and elevations of the inside bar depend on the degree of the convergence of the estuary. The bar moves seaward, and the bar length decreases with a decrease of the convergence length. River discharge also plays important role on the bar location and dimensions. Good relationships exist between river discharge and the location and elevation of the bar apex. Such relationship would be changed with the change of the estuarine planform.

The bar evolution has significant influences on the hydrological regime. The erosion in the upper reach lowers the local low water level and amplifies the tides, whereas the accumulation in the downstream slope of the bar increases the local low water level. Particularly, with the change of the estuarine planform and the seaward movement, the place of the tidal bore occurrence shows a seaward moving and the strength of the tidal bore shows a decreasing trend, explaining the historical and recent evolution of the Qiantang bore. In turn, the morphologically active reach in the estuary strongly influenced by river discharge and the tidal bore also moves seaward.

Data availability

The bathymetric data are available at https://zenodo.org/record/4915584#.YMC0T5yOM2z.

Declaration of Competing Interest

The authors declare that they have no known competing financial interests or personal relationships that could have appeared to influence the work reported in this paper.

Acknowledgments

References

Ahmed, T.S., Egashira, S., Harada, D., Yorozuya, A., 2019. Sediment transportation and sand bar deformation owing to tidal currents in Sittaung River Estuary, Myanmar. J. Jpn Soc. Civ. Eng. (Ser. B1) 75 (2), 1027–1032. https://doi.org/10.2208/jscejhe.75.2_I_1027.

Bartsch-Winkler, S., Lynch, D.K., 1988. Catalog of worldwide tidal bore occurrences and characteristics. USGS Circ. 1022, 1–17.

Bolla Pittaluga, M., Tambroni, N., Canestrelli, A., Slingerland, R., Lanzoni, S., Seminara, G., 2015. Where river and tide meet: the morphodynamic equilibrium of alluvial estuaries. J. Geophys. Res. Earth Surf. 120 https://doi.org/10.1002/2014JF003233.

Bonneton, P., Bonneton, N., Parisot, J.P., Castelle, B., 2015. Tidal bore dynamics in funnel-shaped estuaries. J. Geophys. Res. Oceans 120 (2), 923–941. https://doi.org/10.1002/2014JC010267.

Canestrelli, A., Lanzoni, S., Fagherazzi, S., 2013. One-dimensional numerical modeling of the long-term morphodynamic evolution of a tidally-dominated estuary: the lower

Fly River (Papua New Guinea). Sediment. Geol. 301, 107–119. https://doi.org/10.1016/j.sedgeo.2013.06.009.

Chanson, H.B., 2011. Two-phase flow in hydraulic jumps at large Froude number. J. Hydraul. Eng. 137 (4), 451–460. https://doi.org/10.1061/(ASCE)HY.1943-7900.0000323.

Chanson, H., 2012. Tidal Bores, Aegir, Eagre, Mascaret, Pororoca: Theory and Observations. World Science, Singapore.

Chen, J.Y., Luo, Z.D., Chen, D.C., Xu, H.G., Qiao, P.N., 1964. The formation and historical evolution of the sandbar in Qiantang estuary (in Chinese). Acta Geograph. Sin. 30 (2), 109–113.

Chen, J.Y., Liu, C.Z., Zhang, C.L., Walker, H.J., 1990. Geomorphological development and sedimentation in Qiantang Estuary and Hangzhou Bay. J. Coast. Res. 6 (3), 559–572. https://doi.org/10.2307/4297719.

Chen, S.M., Han, Z.C., Hu, G.J., 2006. Impact of human activities on the river reach in the Qiantang Estuary (in Chinese with English abstract). J. Sediment. Res. 4, 61–67.

Chien, N., Sie, H.S., Chow, C.T., Lee, Q.P., 1964. The fluvial processes of the big sand bar inside the Chien Tang Chiang Estuary (in Chinese with English abstract). Acta Geograph. Sin. 30 (2), 124–142.

Choi, K., Kim, D., Jo, J., 2020. Morphodynamic evolution of the macrotidal Sittaung River estuary, Myanmar: tidal versus seasonal controls. Mar. Geol. 430, 106367. https://doi.org/10.1016/j.margeo.2020.106367.

Dai, Z.J., 2021. Changjiang Riverine and Estuarine Hydro-Morphodynamic Processes: In the Context of Anthropocene Era. Springer.

Dai, Z.J., Liu, J.T., Xie, H.L., Shi, W.Y., 2014. Sedimentation in the outer Hangzhou Bay, China: the influence of Changjiang sediment load. J. Coast. Res. 30, 1218–1225. https://doi.org/10.2112/jcoastres-d-12-00164.1.

Dai, Z.J., Fagherazzi, S., Mei, X., Gao, J., 2016. Decline in suspended sediment concentration delivered by the Changjiang (Yangtze) river into the East China Sea between 1956 and 2013. Geomorphology 268, 123–132. https://doi.org/10.1016/j.geomorph.2016.06.009.

Dai, Z.J., Mei, X., Darby, S.E., Lou, Y., Li, W., 2018. Fluvial sediment transfer in the Changjiang (Yangtze) river-estuary depositional system. J. Hydrol. 566, 719–734. https://doi.org/10.1016/j.jhydrol.2018.09.019.

Dalrymple, R.W., Choi, K., 2007. Morphologic and facies trends through the fluvial–marine transition in tide-dominated depositional systems: a schematic framework for environmental and sequence-stratigraphic interpretation. Earth Sci. Rev. 81 (3), 135–174. https://doi.org/10.1016/j.earscirev.2006.10.002.

Dam, G., Van der Wegen, M., Labeur, R., Roelvink, D., 2016. Modeling centuries of estuarine morphodynamics in the Western Scheldt estuary. Geophys. Res. Lett. 43 (8), 3839–3847. https://doi.org/10.1002/2015GL066725.

De Ridder, M.P., 2017. The Tidal Bore in the Sittaung River - a Sensitivity Analysis of the Propagation. Unpublished master thesis. The Delft University of Technology.

Deltares, 2016. User Manual Delft3d-Flow: Simulation of Multi-Dimensional Hydrodynamic Flows and Transport Phenomena, Including Sediments.

Dijkstra, Y.M., Schuttelaars, H.M., Schramkowski, G.P., Brouwer, R.L., 2019. Modeling the transition to high sediment concentrations as a response to channel deepening in the Ems River Estuary. J. Geophys. Res. Oceans 124, 1578–1594. https://doi.org/10.1029/2018JC014367.

Dolgopolova, E.N., 2013. The conditions for tidal bore formation and its effect on the transport of saline water at river mouths. Water Resour. 40 (1), 16–30. https://doi.org/10.1134/S0097807813010028.

Dyer, K.R., 1997. Estuaries - Physical Introduction. John Wiley and Sons, Chichester.

ECCHE (Editorial Committee for Chinese Harbors and Embayments), 1992. Chinese Harbours and Embayments (Part V, in Chinese). China Ocean Press, Beijing.

Fan, D.D., Tu, J.B., Shang, S., Cai, G.F., 2014. Characteristics of tidal-bore deposits and facies associations in the Qiantang Estuary, China. Mar. Geol. 348, 1–14. https://doi.org/10.1016/j.margeo.2013.11.012.

Fan, D.D., Tu, J.B., Shang, S., Chen, L.L., Zhang, Y., 2016. Morphodynamics and sedimentary facies in a tidal-fluvial transition with tidal bores (the middle Qiantang Estuary, China). In: Tessier, B., Reynaud, J.Y. (Eds.), Contribution to Modern and Ancient Tidal Sedimentology: Proceedings of the Tidalites 2012 Conference, 48, pp. 75–92. IAS Special Publication.

Friedrichs, C.T., Aubrey, D.G., 1994. Tidal propagation in strongly convergent channels. J. Geophys. Res. 99 (C2), 3321–3336. https://doi.org/10.1029/93JC03219.

Gao, S., Wang, Y.P., 2008. Material fluxes from the Changjiang River and their implications on the adjoining continental shelf ecosystem. Cont. Shelf Res. 28, 1490–1500. https://doi.org/10.1016/j.csr.2007.02.010.

Geleynse, N., Storms, J.E.A., Walstra, D.J.R., Jagers, H.R.A., Wang, Z.B., Stive, M.J.F., 2011. Controls on river delta formation; insights from numerical modelling. Earth Planet. Sci. Lett. 302 (1–2), 217–226. https://doi.org/10.1016/j.epsl.2010.12.013.

Godin, G., 1985. Modification of river tides by the discharge. J. Waterw. Port Coast. Ocean Eng. 111 (2), 257–274. https://doi.org/10.1061/(ASCE)0733-950X(1985)111:2(257).

Guo, L.C., Van der Wegen, M., Roelvink, J.A., He, Q., 2014. The role of river flow and tidal asymmetry on 1-D estuarine morphodynamics. J. Geophys. Res. Earth Surf. 119, 2315–2334. https://doi.org/10.1002/2014JF003110.

Han, Z.C., Dai, Z.H., Li, G.B., 2003. Regulation and Exploitation of Qiantang Estuary (in Chinese). China Water Power Press, Beijing.

Hibma, A., Stive, M.J.F., Wang, Z.B., 2004. Esturine morphodynamics. Coast. Eng. 51, 765–778. https://doi.org/10.1016/j.coastaleng.2004.07.008.

Hoitink, A.J.F., Jay, D.A., 2016. Tidal river dynamics: implications for deltas. Rev. Geophys. 54, 240–272. https://doi.org/10.1002/2015RG000507.

Hoitink, A.J.F., Wang, Z.B., Vermeulen, B., Huismans, Y., Kastner, K., 2017. Tidal controls on river delta morphology. Nat. Geosci. 10, 637–645. https://doi.org/10.1038/ngeo3000.

Hu, P., Han, J.J., Li, W., Sun, Z.L., He, Z.G., 2018. Numerical investigation of a sandbar formation and evolution in a tide-dominated estuary using a hydro-sediment-morphodynamic model. Coast. Eng. J. 60 (4), 466–483. https://doi.org/10.1080/21664250.2018.1529263.

Jin, G., Zeng, J., Tang, Z., Hu, C., 2020. Variation trends of tidal characteristics in the Qiantang River Estuary and cause analysis (in Chinese with English abstract). Mar. Sci. Bull. 39 (4), 456–463.

Lanzoni, S., Seminara, G., 1998. On tide propagation in convergent estuaries. J. Geophys. Res. 103 (C13), 30793–30812. https://doi.org/10.1029/1998JC900015.

Leonardi, N., Canestrelli, A., Sun, T., Fagherazzi, S.E., 2013. Effect of tides on mouth bar morphology and hydrodynamics. J. Geophys. Res. 118, 4169–4183. https://doi.org/10.1002/jgrc.20302.

Li, G.B., Dai, Z.H., 1986. Fluvial processes and reclamation of the Qiantang Estuary. Int. J. Sediment. Res. 1 (1), 56–66.

Lin, B.Y., 2008. *Characteristics of Qiantang Bore* (in Chinese). Chinese Ocean Press, Beijing.

Luan, H.L., Ding, P.X., Wang, Z.B., Yang, S.L., Lu, J.Y., 2018. Morphodynamic impacts of large-scale engineering projects in the Yangtze River delta. Coast. Eng. 141, 1–11. https://doi.org/10.1016/j.coastaleng.2018.08.013.

Mei, X., Dai, Z., Wei, W., Li, W., Wang, J., Sheng, H., 2018. Secular bathymetric variations of the North Channel in the Changjiang (Yangtze) Estuary, China, 1880-2013: causes and effects. Geomorphology 303, 30–40. https://doi.org/10.1016/j.geomorph.2017.11.014.

Milliman, J.D., Farnsworth, K.L., 2011. River Discharge to the Coastal Ocean: A Global Synthesis. Cambridge University Press, Cambridge.

Milliman, J.D., Shen, H.T., Yang, Z.S., Robert, H.M., 1985. Transport and deposited of river sediment in the Changjiang estuary and adjacent continental shelf. Cont. Shelf Res. 4, 37–45. https://doi.org/10.1016/0278-4343(85)90020-2.

Nienhuis, J.H., Hoitink, A.J.F., Törnqvist, T.E., 2018. Future change to tide-influenced deltas. Geophys. Res. Lett. 45, 3499–3507. https://doi.org/10.1029/2018GL077638.

Nnafie, A., Van Oyen, T., De Maerschalck, B., Van der Vegt, M., Van der Wegen, M., 2018. Estuarine channel evolution in response to closure of secondary basins: an observational and morphodynamic modeling study of the Western Scheldt Estuary. J. Geophys. Res. Earth Surf. 123 (1), 167–186. https://doi.org/10.1002/2017jf004364.

Nnafie, A., Swart, H.E., De Maerschalck, B., Van Oyen, T., Van der Vegt, M., Van der Wegen, M., 2019. Closure of secondary basins causes channel deepening in estuaries with moderate to high friction. Geophys. Res. Lett. 46 (22), 13209–13216. https://doi.org/10.1029/2019gl084444.

Pan, C.H., Han, Z.C., 2017. Research on Conservation and Regulation of Qiantang Estuary (in Chinese). China Water Power Press, Beijing.

Pan, C.H., Huang, W.R., 2010. Numerical modeling of suspended sediment transport affected by tidal bore in Qiantang Estuary. J. Coast. Res. 26 (6), 1123–1132. https://doi.org/10.2307/40928851.

Pan, C.H., Lu, H.Y., Zeng, J., 2008. Characteristic and numerical simulation of tidal bore in Qiantang River (in Chinese with English abstract). Hydro-Sci. Eng. 2, 1–9.

Partheniades, E.A., 1965. Erosion and deposition of cohesive soils. J. Hydraul. Div. 91 (HY1), 4204. https://doi.org/10.3109/15622970109026808.

Peregrine, D.H., 1966. Calculations of the development of an undular bore. J. Fluid Mech. 25, 321–330. https://doi.org/10.1017/S0022112066001678.

Pye, K., Blott, S.J., 2014. The geomorphology of UK estuaries: the role of geological controls, antecedent conditions and human activities. Estuar. Coast. Shelf Sci. 150, 196–214. https://doi.org/10.1016/j.ecss.2014.05.014.

Savenije, H.H.G., 2012. Salinity and Tides in Alluvial Estuaries (Second Completely Revised Edition). https://salinityandtides.com/.

Shimozono, T., Tajima, Y., Akamatsu, S., Matsuba, Y., Kawasaki, A., 2019. Large-scale channel migration in the Sittang River Estuary. Sci. Rep. 9, 9862. https://doi.org/10.1007/978-981-15-0291-0_163.

Todeschini, I., Toffolon, M., Tubino, M., 2008. Long-term morphological evolution of funnel-shape tide-dominated estuaries. J. Geophys. Res. 113 https://doi.org/10.1029/2007JC004094. C05005.

Townend, I., 2012. The estimation of estuary dimensions using a simplified form model and the exogenous controls. Earth Surf. Process. Landf. 37 (15), 1573–1583. https://doi.org/10.1002/esp.3256.

Tu, J.B., Fan, D.D., Voulgaris, G., 2021. Field observations of turbulence, sediment suspension, and transport under breaking tidal bores. Mar. Geol. 437 (3), 106498. https://doi.org/10.1016/j.margeo.2021.106498.

Van der Wegen, M., Jaffe, B.E., 2014. Processes governing decadal-scale depositional narrowing of the major tidal channel in San Pablo Bay, California, USA. J. Geophys. Res. Earth Surf. 119 https://doi.org/10.1002/2013JF002824.

Van der Wegen, M., Roelvink, J., 2008. Long-term morphodynamic evolution of a tidal embayment using a two-dimensional, process-based model. J. Geophys. Res. Oceans 113 (C3). https://doi.org/10.1029/2006JC003983.

Van der Wegen, M., Roelvink, J.A., 2012. Reproduction of estuarine bathymetry by means of a process-based model: Western Scheldt case study, the Netherlands. Geomorphology 179, 152–167. https://doi.org/10.1016/j.geomorph.2012.08.007.

Van Maren, D.S., Winterwerp, J.C., Vroom, J., 2015. Fine sediment transport into the hyper-turbid lower Ems River: the role of channel deepening and sediment-induced drag reduction. Ocean Dyn. 65 (4), 589–605. https://doi.org/10.1007/s10236-015-0821-2.

Van Rijn, L.C., 1993. Principles of Sediment Transport in Rivers, Estuaries and Coastal Seas. Aqua Publication, Amsterdam.

Wang, Z.B., Louters, T., De Vriend, H.J., 1995. Morphodynamic modelling of a tidal inlet in the Wadden Sea. Mar. Geol. 126, 289–300. https://doi.org/10.1016/S0278-4343(02)-00134-6.

Wang, Z.B., Jeuken, M., Gerritsen, H., De Vriend, H.J., Kornman, B., 2002. Morphology and asymmetry of the vertical tide in the Westerschelde estuary. Cont. Shelf Res. 22 (17), 2599–2609. https://doi.org/10.1016/S0278-4343(02)00134-6.

Wang, Z.B., Van Maren, D.S., Ding, P.X., Yang, S.L., Van Prooijen, B.C., de Vet, P.L.M., Winterwerp, J.C., De Vriend, H.J., Stive, M.J.F., He, Q., 2015. Human impacts on morphodynamic thresholds in estuarine systems. Cont. Shelf Res. 111, 174–183. https://doi.org/10.1016/j.csr.2015.08.009.

Xie, D.F., Wang, Z.B., Gao, S., de Vriend, H.J., 2009. Modeling the tidal channel morphodynamics in a macro-tidal embayment, Hangzhou Bay, China. Cont. Shelf Res. 29, 1757–1767. https://doi.org/10.1016/j.csr.2009.03.009.

Xie, D.F., Pan, C.H., Wu, X., Gao, S., Wang, Z.B., 2017a. The variations of sediment transport patterns in the outer Changjiang Estuary and Hangzhou Bay over the last 30 years. J. Geophys. Res. Oceans 122, 2999–3020. https://doi.org/10.1002/2016JC012264.

Xie, D.F., Gao, S., Wang, Z.B., Pan, C.H., Wu, X., Wang, Q., 2017b. Morphodynamic modeling of a large inside sandbar and its dextral morphology in a convergent estuary: Qiantang Estuary, China. J. Geophys. Res. Earth Surf. 122 (8), 1553–1572. https://doi.org/10.1002/2017JF004293.

Xie, D.F., Pan, C.H., Wu, X., Gao, S., Wang, Z.B., 2017c. Local human activities overwhelm decreased sediment supply from the Changjiang River: continued rapid accumulation in the Hangzhou Bay-Qiantang Estuary system. Mar. Geol. 392, 66–77. https://doi.org/10.1016/j.margeo.2017.08.013.

Xie, D.F., Pan, C.H., Gao, S., Wang, Z.B., 2018. Morphodynamics of the Qiantang Estuary, China: controls of river flood events and tidal bores. Mar. Geol. 406, 27–33. https://doi.org/10.1016/j.margeo.2018.09.003.

Yang, S.L., Milliman, J.D., Li, P., Xu, K.H., 2011. 50,000 dams later: erosion of the Yangtze River and its delta. Glob. Planet. Chang. 75, 14–20. https://doi.org/10.1016/j.gloplacha.2010.09.006.

Yu, Q., Wang, Y.W., Gao, S., Flemming, B., 2012. Modeling the formation of a sand bar within a large funnel-shaped, tide-dominated estuary: Qiantangjiang Estuary, China. Mar. Geol. 299–302, 63–76. https://doi.org/10.1016/j.margeo.2011.12.008.

Zeng, J., Chen, G., Pan, C.H., Zhang, Z.Y., 2017. Effect of dike line adjustment on the tidal bore in the Qiantang Estuary, China. J. Hydrodyn. 29 (3), 452–459. https://doi.org/10.1016/S1001-6058(16)60756-4.

Zhang, W., Ruan, X., Zheng, J., Zhu, Y., Wu, H., 2010. Long-term change in tidal dynamics and its cause in the Pearl River Delta, China. Geomorphology 120 (3–4), 209–223. https://doi.org/10.1016/j.geomorph.2010.03.031.

Zhang, X., Dalrymple, R.W., Yang, S.Y., Lin, C.M., Wang, P., 2015. Provenance of Holocene sediments in the outer part of the Paleo-Qiantang River estuary, China. Mar. Geol. 366, 1–15. https://doi.org/10.1016/j.margeo.2015.04.008.Zhang.

Zhang, X.D., Fan, D., Yang, Z., Xu, S., Chi, W., Wang, H., 2020a. Sustained growth of river-mouth bars in the vulnerable Changjiang Delta. J. Hydrol. 590, 125450. https://doi.org/10.1016/j.jhydrol.2020.125450.

Zhang, S., Pan, C.H., Cheng, W.L., 2020b. Effect of dike line adjustment on the tidal bore in the Qiantang Estuary, China (in Chinese with English abstract). Coast. Eng. 38 (1), 130–139.

Zhang, X., Lin, C.M., Dalrymple, R.W., Gao, S., Li, Y.L., 2014. Facies architecture and depositional model of a macrotidal incised-valley succession (Qiantang River estuary, eastern China), and differences from other macrotidal systems. Geol. Soc. Am. Bull. 126 (3–4), 499–522. https://doi.org/10.1130/B30835.1.

Zhou, Z., Coco, G., Townend, I., et al., 2017. Is "morphodynamic equilibrium" an oxymoron. Earth Sci. Rev. 165, 257–267. https://doi.org/10.1016/j.earscirev.2016.12.002.

Zhou, Z., Coco, G., Townend, I., Gong, Z., Wang, Z.B., Zhang, C.K., 2018. On the stability relationships between tidal asymmetry and morphologies of tidal basins and estuaries. Earth Surf. Process. Landf. 43 (9), 1943–1959. https://doi.org/10.1002/esp.4366.

Zou, Z.N., Shen, Y.M., 2017. Influence of the reclamation project at Qiantang estuary on the hydrodynamics and water environment in Hangzhou bay (in Chinese with English abstracyt). Port Waterw. Eng. 1, 26–33.